Cu-doped CdS QDs for sensitisation in solar cell

Abhigyan Ganguly[1] ✉, *Siddhartha S. Nath*[2], *Madhuchhanda Choudhury*[1]

[1]*Department of ECE, National Institute of Technology, Silchar 788 010, Assam, India*
[2]*Central Instrument Laboratory, Assam University, Silchar 788 011, Assam, India*
✉ *E-mail: abhigyanganguly666@gmail.com*

Published in Micro & Nano Letters; Received on 16th November 2017; Revised on 26th March 2018; Accepted on 25th April 2018

Copper (Cu)-doped cadmium sulphide (CdS) quantum dots (QDs) sensitised zinc oxide photoelectrodes have been fabricated for a solar cell (SC). For the synthesis of QDs, simple chemical methods have been adapted and the QDs were prepared on poly-vinyl alcohol capping agent. The influences of doping on structural properties of QDs have been studied using X-ray diffraction analysis and transmission electron microscopy images. Ultraviolet–visible absorption spectroscopy reveals an enhanced optical absorption in doped QDs. The photovoltaic performance of the Cu-doped CdS QDs was studied by measuring the current density–voltage (J–V) characteristics of the fabricated SC. An enhanced photo-conversion efficiency was observed in doped CdS QDs compared with the undoped QDs sensitised SC.

1. Introduction: In recent times, quantum dot sensitised solar cells (QDSSCs) have attracted a lot of attention of researchers in the field of photovoltaics due to their simple fabrication and their improved photovoltaic efficiency. QDs are used as sensitising layer, deposited over a wide bandgap semiconductor layer typically titanium dioxide or zinc oxide (ZnO) [1]. QDs are zero-dimensional semiconductors that are spatially confined in all three dimensions. Owing to the spatial confinement, QDs have a unique set of optical and electrical properties such as size tunable bandgap, larger surface to volume ratio, multiple exciton generation, and large absorption and extinction coefficients [2]. Among various semiconductor QDs such as cadmium sulphide (CdS) [3], lead(II) sulphide (PbS) [4], cadmium selenide [5], indium phosphide [6] and cadmium telluride [7] which are generally used in QDSSCs, CdS is the most commonly used semiconductor QD material used as sensitisers on the wide bandgap ZnO oxide layer. Both of them are wide bandgap material belonging to II–VI group and the ZnO–CdS system possesses a higher carrier lifetime for photo-generated electrons and holes compared with other oxide-QD combinations [8]. Fig. 1*a* shows the general structure of a QDSSC on FTO glass plate and Fig. 1*b* shows the working of QDSSC.

Doping of QDs with metal ions is considered as one of the methods for increasing the efficiency of SSCs. Doping of nanomaterials with suitable dopant alters the optical as well as electrical properties of semiconductor QDs [9]. The dopant ions create extra electronic states in the bandgap region of QDs, which alters the charge separation and recombination dynamics in the QDSSCs [10]. Doping introduces crystal defects and intermediate energy states in the forbidden energy gap, which alters the optical properties of QDs. In the present investigation, the effect of Cu^{2+} doping in CdS QD is studied as a SC sensitiser in a ZnO–CdS:Cu-based QDSSC. Copper (Cu) has a unique electronic configuration ([Ar] $4s^2 3d^{10}$) and quite different from that predicted from the periodic table. Cu loses the s electrons before losing the d electrons [11]. In neutral atoms, the ns and $(n-1)$d orbitals are very close in energy, with the ns orbitals slightly lower in energy. However, for Cu ions, there is an apparent shifting of energies between the ns and $(n-1)$d orbitals. The energy of the $(n-1)$d orbitals is significantly less than that of the ns electrons. Therefore in Cu ion, the highest-energy electron, which is the ns electron, is removed first. This phenomenon causes an enhancement in electron conduction resulting in an improved current density (J_{sc}) in Cu-doped PbS QDSSC. A simple one pot synthesis chemical method is adopted in the synthesis of pure CdS and Cu-doped CdS QDs on poly-vinyl alcohol (PVA) matrix. PVA capping layer restricts the growth of QDs during the synthesis process, while not itself participating in the chemical reaction. The PVA is a soluble polymer; the precipitated QDs can be easily separated by repeated washing of the precipitate using distilled water [12]. A simple sol–gel-based dip coating technique has been utilised for QDSSC fabrication. An improved absorption and current–voltage characteristic for Cu^{2+}-doped QD sensitising layer and thereby highly improved efficiency is reported.

2. Experimental results: To synthesise CdS QDs by chemical route via one pot synthesis, at room temperature, 0.43 g of PVA is dissolved into 100 ml double distilled water to make 0.1 M solution. This mixture is taken in a three-necked flask fitted with thermometer pocket and N_2 inlet. The solution is stirred by using a magnetic stirrer at a 200 rpm at a constant temperature of 80°C for 3 h until a transparent, viscous solution of PVA is obtained. Similarly, 0.1 M cadmium chloride ($CdCl_2$) solution is made by dissolving 5.03 g of $CdCl_2$ in 25 ml double distilled water. The solutions are degassed by passing N_2 for 3 to 4 h. Next, PVA solution and $CdCl_2$ solution have been mixed and few drops of nitric acid are added to the mixture followed by moderate stirring. About 0.2 g sodium sulphide (Na_2S) is mixed in 25 ml of distilled water to make 0.1 M of an aqueous solution of Na_2S. Na_2S is put into the mixture slowly by means of a dropper unless the whole solution turns yellow. The solution is separated into three separate flasks and 2, 4 and 6% copper(II) chlorides (by weight) were added in three of them, respectively, until the solution turns bluish-green. The solutions are kept in a dark chamber at room temperature for 10 h for its stabilisation followed by filtering out precipitate from the solutions and washing it for three times with deionised water.

To prepare the QDSSCs, zinc accetate and NaOH was mixed in ethanol to obtain ZnO, which was then deposited on four separate conductive Flourine-doped Tin Oxide (FTO)-coated glass (resistivity <10 Ω/sq) by using tape template method and doctor's blade technique. Then, they are heated at 80°C and air annealed at 450°C. Next, the four ZnO-coated glass plates were dipped coated by immersing it in the previously prepared CdS QD solutions of different doping concentrations (0, 2, 4 and 6% by weights, respectively), for around 60 s each to form CdS QD layer on the oxide by chemical bath deposition. A polysulphide electrolyte solution was prepared by adding 2 M of Na_2S and 3 M S in deionised water. Few drops of polysulphide solution are then added on the ZnO–CdS-deposited FTO glass plates and then

doi: 10.1049/mnl.2017.0816

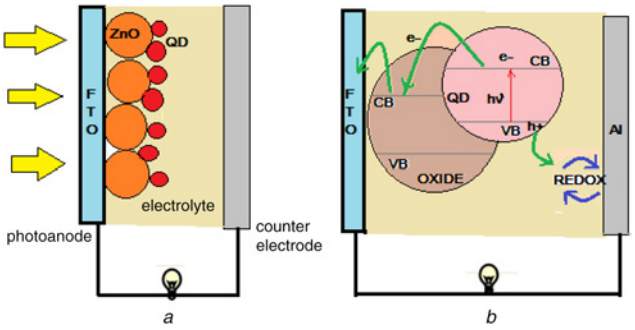

Fig. 1 *General structure of a QDSSC*
a General structure
b Working of a typical QDSSC

Table 1 Data from XRD spectra

QD sample	Diffraction angle 2θ, deg	W, radian	Crystalline plane	Size $D=0.9\lambda/W\cos\theta$, nm	Average size, nm
CdS	26	0.0262	111	5.4	6.8
	28	0.0209	101	6.8	
	31	0.0175	200	8.1	
CdS:	27	0.0244	111	5.8	6.03
Cu	28.4	0.0210	101	6.8	
(2%)	31.6	0.0262	200	5.5	
CdS:	27	0.0175	111	8.17	7.4
Cu	28.8	0.0244	101	5.8	
(4%)	32	0.0175	200	8.2	
CdS:	27	0.0262	111	5.45	7.3
Cu	28.8	0.0174	101	8.2	
(6%)	32	0.0175	200	8.3	

they are sandwiched with a thin aluminium plate, with thin glass cover slip spacers in between. The aluminium plate acts as a counter electrode and it is held together with the glass plate by using scotch tapes and clips. Two metal crocodile probes were connected one to the FTO plate and another to the aluminium plate.

To understand the nanocharacteristics of prepared QDs, the sample has been tested by ultraviolet–visible (UV–vis) spectrophotometer, X-ray diffraction (XRD) spectrometer and high-resolution transmission electron microscope (HRTEM) (Table 1). UV–vis light absorption spectra were obtained using Perkin-Elmer Lamda 35 UV–vis spectrophotometer. XRD patterns were obtained (Bruker AXS, X-ray source: Cu Kα) and HRTEM (JEM 1000 C XII). Current–voltage relation of the fabricated SCs has been studied by using multimeter (Keithley 2001). Photocurrent is measured under the illumination of a 500 W xenon lamp (100 mW cm^{-2}) with an area of illumination as 0.3 cm^{-2}.

3. Results and discussion: Fig. 2 shows the XRD pattern of pure CdS and Cu-doped CdS QDs. XRD investigation shows that pure CdS shows peaks at 26° (111), 28° (101) and 31° (200). The doping of Cu ions in CdS does not result in any significant difference in the XRD pattern of CdS. A slight shift of peaks in XRD pattern toward higher angle in doped QDs is due to substitution of Cd^{+2} in the crystal lattice by Cu^{+2} ions. The average particle sizes are assessed from diffractograms and the data is given in Table 2. From XRD study, average particle size (crystallite size) is calculated by using Scherrer formula [13]

$$D = 0.9\lambda/W\cos\theta, \tag{1}$$

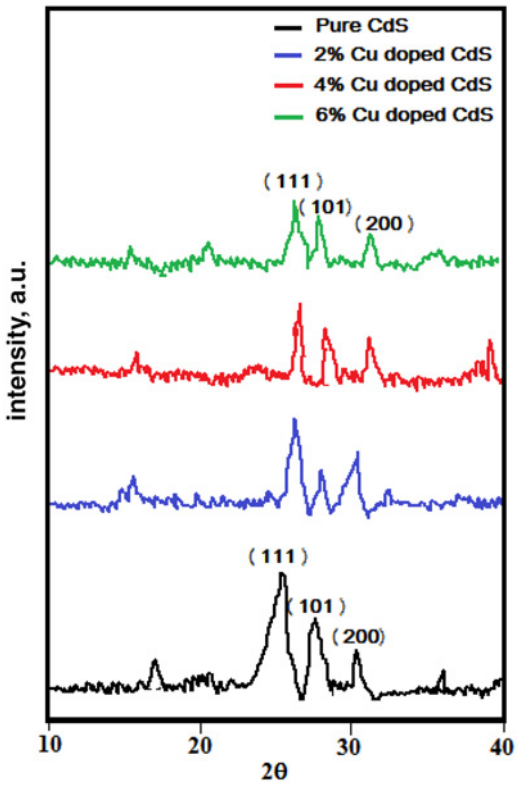

Fig. 2 *XRD pattern for pure CdS and 2, 4 and 5% Cu-doped CdS QDs*

Table 2 Data from absorption spectra

QD sample	Absorption edge, nm	Bandgap, eV	Estimated size, nm
CdS	410	3.02	6.2
CdS:Cu (2%)	400	3.1	5.24
CdS:Cu (4%)	403	3.08	5.5
CdS:Cu (6%)	408	3.04	6

where 'λ' is the wavelength of X-ray (0.1541 nm), 'W' is the full width at half maxima, 'θ' (theta) is the glancing angle and 'D' is the particle diameter (crystallite size). Considering all the peaks (2θ in degrees) in the X-ray diffractogram, the average crystallite (QD) size has been assessed and found to be about 6.8 nm for CdS and 6.03, 7.4 and 7 nm for CdS:Cu at 2, 4 and 6% doping concentrations, respectively.

Fig. 3 shows the optical absorption spectra for undoped as well as Cu-doped CdS QDs. Strong absorbance edge is observed at 410 nm for undoped CdS, and for Cu-doped CdS the absorption edges are observed as 400, 403 and 408 nm for 2, 4 and 6% doping concentrations, respectively. Absorption edge is estimated by drawing tangent [12] to the absorption curve as shown in Fig. 3. Absorption edge marks the wavelength value corresponding to the respective bandgap of the QDs. Absorption edge showed a slight blue shift for doped QDs. This slight shifting in absorption edge can be attributed to the quantum confinement effect produced due to increased nucleation rate with doping as observed previously in other works [14] (Fig. 4 and 5). From the absorbance edge, particle size has been calculated using effective mass approximation [15]

$$E_{gn} - E_{gb} = \frac{\hbar^2\pi^2}{2m^*R^2} \tag{2}$$

where R is the QD radius, E_{gb} is the bulk bandgap, E_{gn} is the QD bandgap, m^* is the effective mass of the specimen, h is Planck's

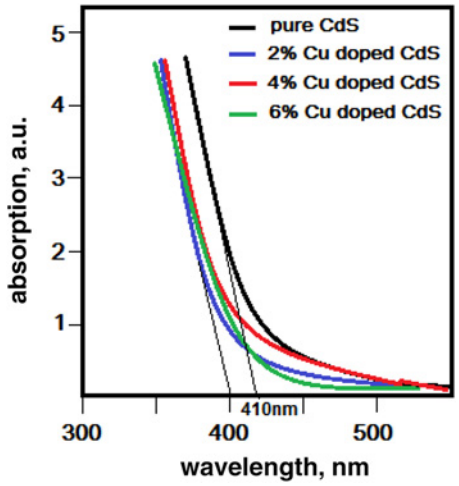

Fig. 3 *UV–vis absorption spectra for pure CdS and 2, 4 and 5% Cu-doped CdS QDs*

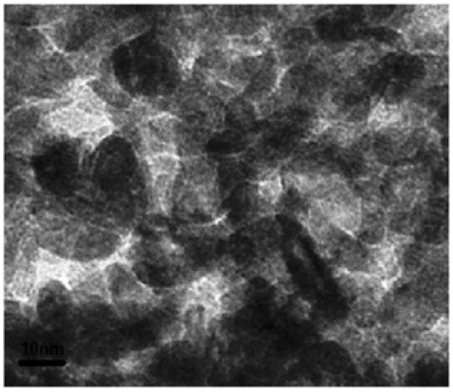

Fig. 4 *HRTEM image of pure CdS QDs*

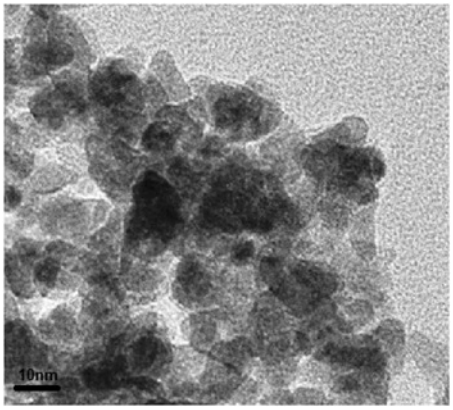

Fig. 5 *HRTEM image of 4% Cu-doped CdS QDs*

constant and h bar is reduced plank's constant, i.e. $h/2\pi$. Here, the bulk bandgap (E_{gb}) for CdS is 2.84 eV and electron effective mass at room temperature is $0.211m_o$ [16]; where m_0 is the electron rest mass. The QD bandgaps (E_{gn}) of the prepared samples as determined from the absorption edge wavelength. Both pure and Cu-doped CdS QD bandgap are found to be around 3 eV and the estimated size for the synthesised QDs for the corresponding bandgap is determined to be around 6 nm. The HRTEM images confirm that the sizes of QDs are around 6 nm as estimated by XRD pattern and absorption

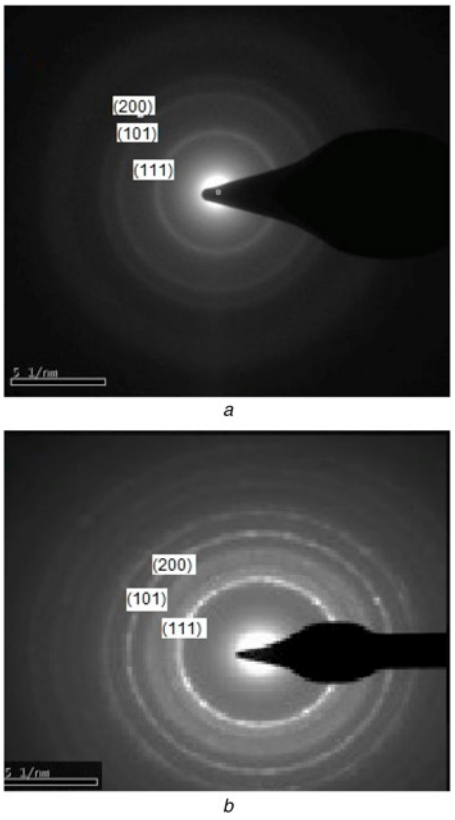

Fig. 6 *SAED pattern of*
a Pure CdS QDs
b 4% Cu-doped CdS QDs

spectroscopy. The selected area electron diffraction pattern (SAED) of the QDs is shown in Fig. 6, where each concentric circle corresponds to different crystalline plane of CdS. From the SAED pattern, it can be clearly observed that the QDs are crystalline in nature. The data from the UV–vis absorption spectroscopy is given in Table 2.

Fig. 7 shows the current density–voltage (J–V) characteristics of the CdS and Cu-doped CdS QD sensitised ZnO thin film-based SCs at different doping concentrations. For studying the SC characteristics, the fabricated devices are illuminated by white light using xenon lamp with illumination area of about 0.3 cm^{-2} and the current density (J) v/s voltage (V) is measured. The short-circuit current density (J_{sc}) and open-circuit voltage (V_{oc}) have been obtained from J–V curves. Fill factor (FF) and power conversion efficiency (η) have been calculated by using the following equations:

$$\mathrm{FF} = \frac{J_{\max} V_{\max}}{J_{sc} V_{oc}} \tag{3}$$

$$\eta = \frac{V_{oc} \times I_{sc} \times \mathrm{FF}}{P_{in}} \tag{4}$$

The SC parameters for both the undoped CdS and the three different concentrations of Cu-doped CdS QDSSCs are shown in Table 3. For the undoped CdS cell 0.99% efficiency was obtained, whereas for the Cu-doped CdS the efficiency values obtained are 1.5, 1.8 and 1.56% for 2, 4 and 6% doping concentrations, respectively. Highest efficiency reaching as high as 1.8% was observed for 4% Cu doping concentration. With increase in doping, that is at 6%, Cu ions create excess of mid-gap states that causes electrons to get trapped and screen it from charge recombination with holes and with the polysulphide electrolyte [10]. This effects the redox operation in higher doping concentrations and causes deterioration in

doi: 10.1049/mnl.2017.0816

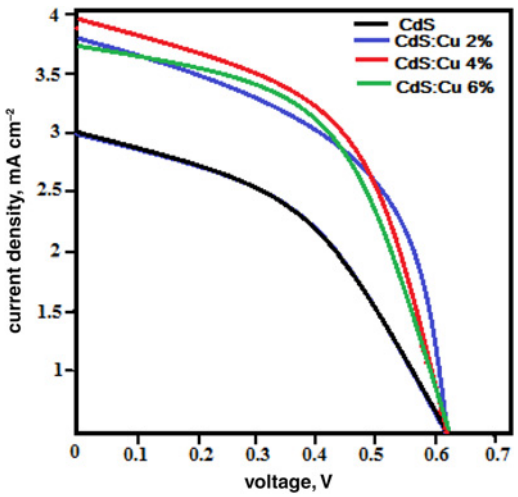

Fig. 7 *Current density–voltage characteristics of ZnO-based QDSSC with CdS and CdS:Cu QD sensitised layer*

Table 3 Photovoltaic parameters of pure CdS and Cu-doped CdS sensitised ZnO SC at different doping concentrations

QD sensitisers	V_{oc}, V	J_{sc}, mA cm^{-2}	FF	η
CdS	0.6	3	0.55	0.99
CdS:Cu (2%)	0.6	3.72	0.67	1.5
CdS:Cu (4%)	0.6	4	0.75	1.8
CdS:Cu (6%)	0.6	3.7	0.70	1.56

overall performance of the doped SCs. On the contrary, previously reported pure CdS QD-based SCs in Chen *et al.* [3] an efficiency was obtained 0.69% and in Singh *et al.* [17] obtained 1.2% efficiency. This results clearly indicates that there is an overall increase in the SC efficiency with Cu^{+2} doping of the CdS sensitising layer.

4. Conclusion: Different concentrations of Cu^{+2}-doped CdS QDs with PVA capping layer are synthesised via chemical method. The XRD pattern shows that the prepared pure CdS and Cu-doped CdS samples have similar crystal structure. The slight shift of diffraction peaks in case of doped samples indicates successful doping of Cu^{+2} in CdS QDs. The size of synthesised QDs is estimated to be within 10 nm from both XRD as well as UV–vis absorption study. HRTEM shows the formation of CdS QDs of size around 10 nm on PVA matrix. The synthesised QDs are introduced as sensitiser in a ZnO thin film SC and the SC parameters were obtained for white light illuminated condition. About 4% Cu^{+2}-doped CdS QDs on ZnO thin films exhibits a highest short-circuit current density (J_{SC}) of about 4 mA/cm^2, an open-circuit voltage (V_{OC}) of 0.6 V, an FF of 0.75 and a highest power conversion efficiency (η) of around 1.8%. For higher doping concentration, the conversion efficiency decreases.

5 References

[1] Semonin O.E., Luther J.M., Beard M.C.: 'Quantum dots for next-generation photovoltaics', *Mater. Today*, 2012, **15**, pp. 508–515

[2] Tian J., Cao G.: 'Control of nanostructures and interfaces of metal oxide semiconductors for quantum dots sensitized solar cells', *J. Phys. Chem. Lett.*, 2015, **6**, (10), pp. 1859–1869

[3] Chen H., Li W., Liu H., *ET AL.*: 'CdS quantum dots sensitized single- and multi-layer porous ZnO nanosheets for quantum dots-sensitized solar cells', *Electrochem. Commun.*, 2011, **13**, pp. 331–334

[4] Wang H., Pedro V.G., Kubo T., *ET AL.*: 'Enhanced carrier transport distance in colloidal PbS quantum-dot-based solar cells using ZnO nanowires', *J. Phys. Chem. C*, 2015, **119**, pp. 27265–27274

[5] Gao B., Shen C., Zhang B., *ET AL.*: 'Green synthesis of highly efficient CdSe quantum dots for quantum-dots-sensitized solar cells', *J. Appl. Phys.*, 2014, **115**, (19), pp. 1931041–1931046

[6] Zaban A., Micic O.I., Gregg B.A., *ET AL.*: 'Photosensitization of nanoporous TiO_2 electrodes with InP quantum dots', *Langmuir*, 1998, **14**, pp. 3153–3156

[7] Lee H.J., Kim D.Y., Yoo J.S., *ET AL.*: 'Anchoring cadmium chalcogenide quantum dots (QD) onto stable oxide semiconductor for QD sensitized solar cells', *Bull. Korean Chem. Soc.*, 2007, **28**, pp. 953–958

[8] Poornima K., Krishnan K.G., Lalitha B., *ET AL.*: 'CdS quantum dots sensitized Cu doped ZnO nanostructured thin films for solar cell applications', *Superlattices Microstruct.*, 2015, **83**, pp. 147–156

[9] Nath S.S., Chakdar D., Gope G., *ET AL.*: 'Green luminescence of ZnS and ZnS:Cu quantum dots embedded in zeolite matrix', *J. Appl. Phys.*, 2009, **105**, (09), pp. 4305–4309

[10] Santra P.K., Kamat P.V.: 'Mn-doped quantum dot sensitized solar cells: a strategy to boost efficiency over 5%', *J. Am. Chem. Soc.*, 2012, **134**, pp. 2508–2511

[11] Khanna S.N., Ashman C., Rao B.K., *ET AL.*: 'Geometry electronic structure and energetic of Cu-doped aluminium clusters', *J. Chem. Phys.*, 2001, **114**, p. 9792

[12] Nath S.S., Choudhury M., Chakdar D., *ET AL.*: 'Acetone sensing property of ZnO quantum dots embedded on PVP', *Sens. Actuators B*, 2010, **148**, pp. 353–357

[13] Sahay P.P, Tewari S., Nath R.K.: 'Optical and electrical studies on spray deposited ZnO thin films', *Cryst. Res. Technol.*, 2007, **42**, pp. 723–729

[14] Devi L.S., Devi K.N., Sharma B.I., *ET AL.*: 'Influence of Mn doping on structural and optical properties of CdS nanoparticles', *Indian J. Phys.*, 2014, **88**, (5), pp. 477–482

[15] Chukwuocha E.O., Onyeaju M.C., Harry T.S.: 'Theoretical studies on the effect of confinement on quantum dots using the Brus equation', *World J. Condens. Matter. Phys.*, 2012, **2**, pp. 96–100

[16] Jun H.K., Careem M.A., Arof A.K.: 'Performances of some low-cost counter electrode materials in CdS and CdSe quantum dot-sensitized solar cells', *Nanoscale Res. Lett.*, 2014, **9**, (1), pp. 69–76

[17] Singh N., Mehera R.M., Kapoor A., *ET AL.*: 'ZnO based quantum dot sensitized solar cell using CdS quantum dots', *J. Renew. Sustain. Energy*, 2012, **4**, p. 013110-10, doi: 10.1063/1.3683531